Michael C. Coniglio[*1] and Stephen F. Corfidi[2]
[1]NOAA/National Severe Storms Laboratory, Norman, OK
[2]NOAA/Storm Prediction Center, Norman, OK

1. INTRODUCTION

Forecasting the details of mesoscale convective systems (MCSs) (Zipser 1982) continues to be a difficult problem. Recent advances in numerical weather prediction models and computing power have allowed for explicit real-time prediction of MCSs over the past few years, some of which have supported field programs (Davis et al. 2004) and a collaborative experiment between researchers and forecasters at the Storm Prediction Center (SPC) (Kain et al. 2005). While these numerical forecasts of MCSs are promising, the utility of these forecasts and how to best use the capabilities of the high-resolution models in support of operations is unclear, especially from the perspective of the Storm Prediction Center (SPC) (Kain et al. 2005). Therefore, refining our knowledge of the interactions of MCSs with their environment remains central to advancing our near-term ability to forecast MCSs.

a. MCS speed

The speed of MCSs plays a significant role in both the likelihood of producing damaging surface winds and their longevity, but accurate estimates of MCS motion prior to MCS initiation are difficult at best. It is well known that the speed of a storm-induced cold pool can be estimated theoretically through density current dynamics (see Bryan et al. 2005), but the observations required to make these calculations aren't routinely available. Even if calculations of this type were available, predicting MCS speed is inherently nonlinear because it requires anticipating how the environment and system will interact to affect the advection and propagation of the system itself. This often leads to significant along-line and temporal variability of speeds associated with the leading line motion.

The speed of MCSs plays a significant role in both the production of damaging surface winds and its longevity, but accurate estimates of MCS motion prior to MCS initiation are difficult at best. Predicting MCS speed is inherently nonlinear because it requires anticipating how the environment and system will interact to affect the advection and propagation of the system itself. Useful estimates of the advective component of MCS motion can be provided by the mean cloud-layer wind (see Corfidi 2003 and Cohen et al. 2005 elsewhere in this volume). But forecasting MCS propagation is more problematic since the cold pool of air that results from the evaporation/melting of precipitation always interacts with the environment and the ensuing regions of convergence along the cold pool can greatly influence the propagation of the parent MCS (Corfidi 2003).

b. MCS maintenance

Predicting MCS maintenance is fraught with challenges such as understanding how deep convection is sustained through system/environment interactions (Weisman and Rotunno 2004, Coniglio et al. 2004, Coniglio et al. 2005), how pre-existing mesoscale features influence the system (Fritsch and Forbes 2001, Trier and Davis 2005), and how the disturbances generated by the system itself can alter the system structure and longevity (Parker and Johnson 2004c).

From an observational perspective, Evans and Doswell (2001) suggest that the strength of the mean wind (0-6 km) and its effects on cold pool development and MCS motion plays a significant role in sustaining long-lived forward-propagating MCSs that produce damaging surface winds (derechos) through modifying the relative inflow of unstable air. They also show, however, that a wide range of convective available potential energy (CAPE) and vertical wind shear is found in the environments of derechos, likely reflecting the large spectrum of scales that contribute to the maintenance of the convection in many cases.

Through the use of wind profiler observations and numerical model output, Gale et al. (2002) examine nocturnal MCSs in Iowa to determine predictors of their dissipation. Similar to Evans and Doswell (2001), they find that changes in MCS speed may control its dissipation through changes in low-level storm-relative inflow. However, despite some indications that a decreasing low-level-jet intensity and low-level equivalent potential temperature (θ_e), and it's advection, can be useful in some cases, they did not find robust predictors of MCS dissipation.

[*] *Corresponding author address*: Michael Coniglio, NSSL, 1313 Halley Circle, Norman, OK, 73069; e-mail: Michael.Coniglio@noaa.gov

The analysis of proximity soundings in Coniglio et al. (2004) also shows that CAPE and low-level wind shear varies considerably in derecho environments and that significant wind shear often exists in mid and upper levels in the pre-convective environment. An emphasis of this work is that wind shear over deeper layers than those considered in past idealized modeling studies (Weisman and Rotunno et al. 2004) may be important for the maintenance of these systems, especially when the cold pool is very strong. This result is echoed in Stensrud et al. (2005) and later is this paper. This point may be particularly relevant since observations of cold pools from the BAMEX[1] filed campaign show that cold pools are often deeper than suggested by idealized simulations of convective systems, with the storm-induced cold air usually extending to 3 to 5 km above ground (Bryan et al. 2005).

c. Goals

In order to motivate the examination of observed MCS environments found in section 3, we will briefly examine some newly-developed ideas on the maintenance of MCSs through cold pool/environment interactions in section 2. We focus our attention on the more robust systems that obtain a quasi-linear leading line and tend to produce severe weather and strong cold pools, and therefore, we intend for this discussion to be most applicable to systems that are not strongly tied to frontal-scale forcing (Fritsch and Forbes 2001) or strong low-level jets (Trier and Davis 2005).

Using the ideas presented in section 2 as a guide, the main goal of this work is to examine a large data set of proximity soundings to identify predictors of MCS speed and dissipation through an improved understanding of the observed environments of MCSs and to develop forecast tools based on these predictors. The approach, described in section 3, is to use statistical techniques on the predictors to develop equations for the probability of MCS maintenance and the probability of an MCS reaching a particular speed. The "best" predictors of MCS speed and dissipation and the development of the probability equations are discussed in section 4. Finally, we end the paper with examples of two successes of the probability equations during their application during this past summer at the SPC is discussed in section 5 a discussion of the limitations of the forecasting tools.

2. COLD POOL/ENVIRONMENT INTERACTIONS

As stated above, this study focuses on the class of MCSs that develop strong cold pools and a quasi-linear or arced region of strong convection along their leading edge. For years, researchers have employed idealized convection-resolving numerical models to understand the physical connection between the environmental vertical wind shear, usually the low-level shear, and the behavior of these types of MCSs (see Weisman and Rotunno 2004 for a review). Much of this work emphasizes the importance of the low-level shear to counter the effects of the organized cold thunderstorm outflow (cold pool). Weisman and Rotunno (2004, WR04 hereafter) revisit many years of idealized modeling studies to affirm that surface-based shear distributed to depths greater than 5 km is detrimental to producing strong quasi-2D convective systems by sighting the lessened overall condensation, rainfall, and surface winds, as well as the lack of organized line segments and bow echoes in deep shear noted in their simulations.

Other researchers have looked at the effects of deeper shear on MCSs in more detail. In a set of idealized two-dimensional (2D) simulations of squall lines, Fovell and Daily (1995) examine the effects of shear-layer depth for a fixed value of vertical shear. Although they focus on the temporal behavior of the multicellular updraft cycles, they show that as the shear-layer depth is increased, the model storms become stronger with more upright convective updrafts and longer periods of organized oscillatory behavior despite a decreasing amount of shear over a given low-level layer, contrary to the results of Weisman and Rotunno (2004) for shear-layer depths above 5 km.

A recent set of papers by Parker and Johnson (2004a, b, c) examine the dynamics of quasi-2D convective systems in deep-tropospheric shear. Although their main focus is on the development and effects of the leading stratiform precipitation, they explain the development of a deep, efficient convective overturning through the linear component of the perturbation pressure field, which generates downshear accelerations in mid levels on the upshear sides of the updrafts in positive shear. Fig. 1b displays their conceptual model for the development of this type of deep overturning and the decomposition of the transient pressure forces that account for a significant portion of the net overturning over time. As in some past analytical studies of 2D convection (Shapiro 1992, Moncrieff and Liu 1999), they hypothesize that the shear gives air parcels more upright trajectories and allows them to spend more time in the zone of upward accelerations.

---

[1] BAMEX stands for the Bow Echoes and Mesoscale Convective Vortex (MCV) Experiment, which was a field program that took place between 20 May and 6 July 2003 and was designed to obtain high-density kinematic and thermodynamic observations in and around bow-echo MCSs and MCVs (Davis et al. 2004).
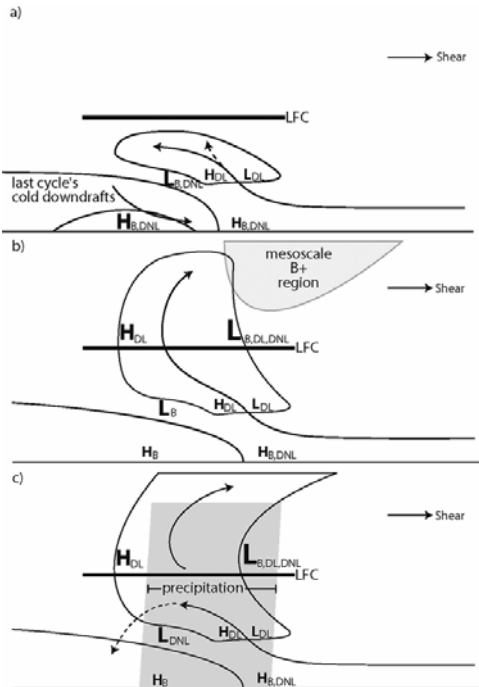
Fig. 1. Schematic depiction of a multicellular cycle within a convective system in deep shear. (a) Development of a fresh updraft at the outflow boundary/gust front; (b) maturation of the overturning updraft; (c) the updraft is cut off from the inflow by precipitation. The cold pool and cloud outlines are shown schematically, along with typical airstreams. The LFC and orientation of the deep tropospheric shear vector are also shown. In (b), the shaded region represents the mesoscale region of positive buoyancy (B+) associated with the line-leading cloudiness. In (c), the shaded region represents the newly developed convective precipitation. Pressure maxima and minima are shown with "H" and "L" characters: their sizes indicate approximate magnitudes and their subscripts indicate the pressure components to which they are attributed, denoting the linear dynamic component (DL), the nonlinear dynamic component (DNL) or the buoyancy component (B). The vertical scale is expanded somewhat below the LFC and contracted somewhat above the LFC (adapted from Parker and Johnson 2004b).

This model of deep convective overturning in deep shear is examined further in Coniglio et al. (2005) through idealized 3D numerical simulations of convective systems in varying amounts of vertical shear in the 5-10 km layer above a fixed amount of low-level shear (20 m s^{-1}/0-5 km). They show quantitatively that the addition of shear above the storm-induced cold pool up to 10 km can allow for much deeper lifting of the overturning air parcels and a much greater percentage of parcels that are lifted to higher levels (Fig. 2). They argue that the deeper shear predisposes the environment to placing a steering level (the level at which the cold pool speed matches the line-normal environmental wind speed) somewhere in mid and upper-levels, which allows the convective regions and the favorable downshear accelerations shown in Fig. 1b

to remain close to the cold pool leading edge facilitating the maintenance of the system as a whole. This lifting is maximized for moderate upper-level shear values (10–15 m s^{-1}) (Fig. 2) and is manifest in quasi-2D regimes as larger, stronger, more upright collections of line segments and bow echoes that persist for longer periods along the leading edge of the cold pool. As the shear becomes stronger over a 10 km layer, more isolated 3D structures become prominent along the cold pool leading edge, but strong line segments and bow echoes can still persist.
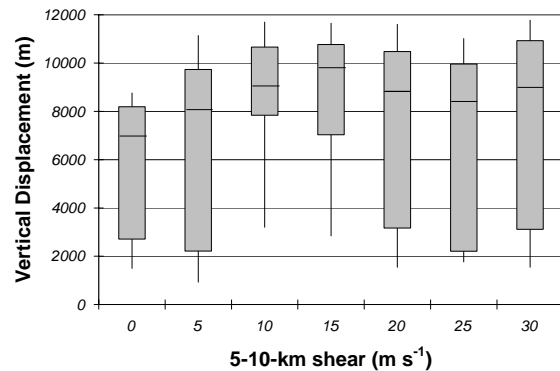

Fig. 2. Distributions of the maximum vertical displacements of several hundred parcels that pass through the deep convective regions of simulated convective systems within various values of 5-10-km shear (all of the simulations had a fixed value of 20 m s^{-1} of shear over 0-5 km). The lines extend to the 10th and 90th percentiles and the boxes enclose the interquartile range (25th and 75th percentiles). The thin lines within each box represent the median (adapted from Coniglio et al. 2005).

Parker and Johnson (2004a) provide a summary of observations of these types of systems in which these processes may have been very important. In addition, the recent Bow Echoes and Mesoscale Convective Vortex Experiment (BAMEX) (Davis et al. 2004) allows for unprecedented observations of the flow structures of strong quasi-linear MCSs. The observed flow structure of the 9-10 June 2003 nocturnal bow echo-MCS event is particularly interesting. The flow structure revealed by high quality multiple Doppler radar analysis suggests that the parcels originating above 2 km are overturning deeply and the parcels below this level are passing through the cold pool region (Fig. 3), similar to the conceptual model shown in Fig. 1. A special sounding taken in the inflow environment (Fig. 4) shows a complex low-level shear profile and a relatively dry surface layer that suggests a decoupling of the surface layer from the high θ_e air at 850 hPa and above. It is intriguing that the mean shear profile in a layer that is based at 850 hPa and extends through the convective cloud layer has significant positive shear (Fig. 4), which suggests that the elevated overturning process and the enhancement in lifting from shear above the cold pool may have been important for this event.
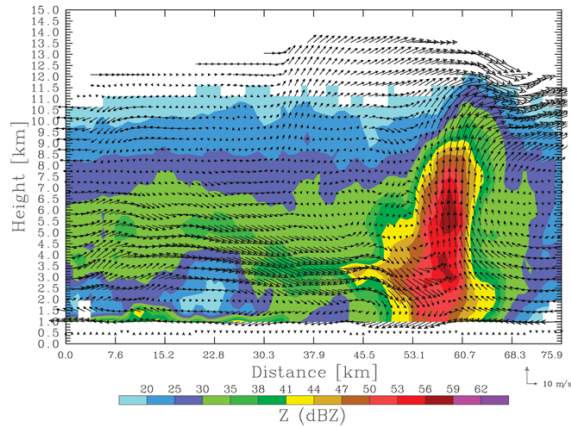
Fig. 3. Cross section from the 10 June bow echo MCS produced from quad-Doppler analysis. Shown are system-relative winds and reflectivity (dbZ) in the vertical plane (from Davis et al. 2004).
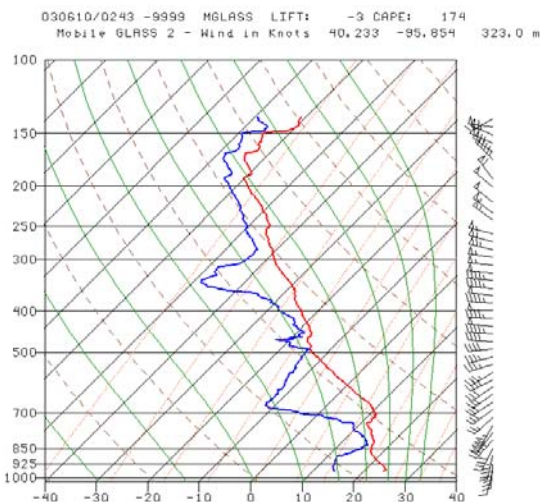
Fig. 4. Special sounding launched at 0243 UTC 10 June in the environment ahead of the bow echo MCS (obtained from http://www.joss.ucar.edu/bamex/catalog).

The recent studies discussed above suggest that physical mechanisms related to upper-level shear are relevant to both quasi 2D and 3D regimes of MCSs and that the low-level shear/cold pool interactions that help to organize the systems and determine the strength of the systems initially (Weisman and Rotunno 2004) do not provide a complete picture of the complex question of MCS structure and maintenance, especially once a strong, organized cold pool and deep mesoscale updrafts become established.

The discussion above leads us to examine the observed environments of MCSs with a more discerning outlook if we are to develop a clearer understanding of their longevity and propagation characteristics and if we are to improve the methods for their prediction. This

paper takes the approach of much past operationally-oriented research by attempting to find environmental parameters that differentiate between MCSs of different speeds and durations by examining observed proximity soundings. The focus is on predicting the speed and maintenance of MCSs on 3-12 hour time scales, which could benefit Day 1 Severe Weather Outlooks, Mesoscale Discussion products, and the issuance of Severe Weather Watches at the Storm Prediction Center (SPC) and short-term forecasts issued by local forecast offices.

3. DEVELOPMENT OF FORECAST TOOLS

a. MCS proximity sounding data set

To develop a data set of MCS events large enough to make statistically important conclusions in a systematic and expeditious manner, we identify MCSs by examining composites of base radar reflectivity for the months of May-August during the seven-year period of 1998-2004. We follow the Parker and Johnson (2000) description of MCSs and focus our attention on the type that have a nearly contiguous quasi-linear or bowed leading edge of reflectivity values at least 35 dbZ at least 100 km in length. While a 100 km long collection of cells could be considered an MCS if it persists for at least 2-3 hours (based on consideration of the Rossby radius of influence; Cotton et al 1989), we only consider events that maintained this spatial configuration for at least 5 continuous hours to focus on the longer-lived systems. From a set of over 600 MCSs of this type that are identified during this period, we identify 269 events in which a radiosonde observation was taken within about 200 km and 3 h of the linear portion of the MCS and displayed no obvious signs of contamination from convection. In addition, only those events that appeared to have their primary inflow sampled by the sounding are included in this tally. We added 79 derecho proximity soundings used in Coniglio et al. (2004) that were identified using a similar procedure for a total of 348 warm-season (May-August) proximity soundings that are used to examine the environments of MCSs in this study.

At the time of the proximity sounding, the appearance and trends of the radar reflectivity data were used to assess subjectively the mean speed and direction of the leading-line MCS motion and the stage of the MCS in its life cycle. The motion is defined based on both a mean along-line motion and a mean motion observed in a 3 hour window centered at the time of the sounding. Within this 3-hour window, the three stages in the MCS lifecycle considered are (1) initial cells prior to MCS development ("initiation"), (2) mature MCS, with strengthening or quasi-steady high reflectivity (50 dBZ or higher) embedded within the nearly contiguous line of 35+ dbZ echoes ("mature"), (3) decaying MCS, with significantly weakened or shrinking areas of high reflectivity, or a loss of system organization and

associated areas of high reflectivity ("dissipation"). If two of these stages are observed within the 3 hour window, the stage that persists the longest in this window is used to define the MCS stage for that sounding.

Since our focus is on forward-propagating systems in this study, the predictors for MCS dissipation are derived from a subset of soundings that sampled the environment ahead of an MCS in which the leading line was moving ≥ 10 m s^{-1} near the sounding time. Although MCSs that move at speeds less than 10 m s^{-1} aren't necessarily physically distinct from faster forward-propagating systems, this helps to ensure that we are including systems with significant cold pools. This produces a subset of 287 soundings that are used in the development of the MCS dissipation predictors. These soundings are then stratified into 76 "initiation", 96 "mature", and 115 "dissipation" soundings based on the appearance and trends of the radar reflectivity at the time of the sounding as described above.

To derive predictors for the speed of MCSs, we remove the dissipation soundings and stratify the remaining 228 soundings according to the speed of the leading line during the organizing and mature stages of the MCSs. These soundings are classified into two groups; the 98 soundings associated with MCS speeds (C) ≥ 18 m s^{-1} and the 130 soundings associated with C < 18 m s^{-1}. We use a speed of 18 m s^{-1} as the break point because operational experience suggests that systems moving faster than this speed have an increased likelihood of producing damaging wind gusts (as long as the storms are rooted in the boundary layer), which is supported by Cohen et al. (2005).

b. Statistical methods

Several hundred variables are calculated that represent various aspects of the kinematic and thermodynamic inflow environment. Although substantial correlations exist among these variables, it is not necessary to make any prior assumptions about which of these variables are the best discriminators. Therefore, we focus on a handful of variables that are found to have the largest statistically significant differences among the MCS categories and focus on those variables that are emphasized previous studies.

To assess the statistical differences, we use the Mann-Whitney test to identify parameters that give the lowest probabilities that the sample means among the two groups in question are the same, which, in the Mann-Whitney approach, is equivalent to the selection of the parameters that produce the largest Z-scores between the two groups (see Wilks 1995 for details). Non parametric tests like the Mann-Whitney test are attractive in this application since there is no requirement to assume an underlying Gaussian distribution to the data sample, which is required in a

parametric method, such as the widely used student's t-test approach (Wilks 1995).

Using the Z-scores as a guide, discriminant analyses are then used to find the number and particular combination of parameters that provide the "best" separation among the two groups in question. This amounts to determining the combination of parameters that produce the highest percentage correctly-grouped soundings. We find that the percentages of correct groupings in the discriminant analyses converged to within 1-2% after the inclusion of only 3 to 4 variables in the analyses, which is a reflection of the substantial correlations.

Once the parameters that best discriminate between two groups are identified, we use logistic regression (Wilks 1995) to develop probability equations for MCS maintenance and for the probability that the leading edge of the MCS will move at speeds ≥ 18 m s^{-1} (35 kts). Logistic regression is a method of producing probability forecasts on a set of binary data (or data within two groups) by fitting parameters to the equation

$$y = \frac{1}{1 + \exp[b_0 + b_1 x_1 + b_2 x_2 + \cdots + b_k x_k]} \quad (1)$$

where y is the fractional probability of one of the groups occurring, k is the number of predictors, x_k refers to the kth predictor, and b_k refers to the kth regression coefficient for each predictor (see Wilks 1995 for more information). Logistic regression is attractive in this context because the predictand is a probability, i.e., it allows for the direct computation of probabilities between two possible outcomes in a set of data.

c. Interpretation of the probability equations

Although we develop three separate categories for the stages in the MCS lifecycle, the first part of section 4 focuses on forecasting the probability of MCS maintenance, which amounts to finding the best predictors between the mature and dissipation soundings. As dictated by the subjective definition of the mature and dissipation categories, the logistic regression equation for the MCS maintenance probabilities is designed to give the probability of a "mature" MCS as defined above. However, given the variability in MCS intensities observed for the mature sample, it is an unavoidable consequence of the experimental design that the intensity of the MCS is not independent of the stage of the MCS. This is because the same predictors that discriminate well between the mature and weakening stages of a particular MCS also appear to discriminate well between MCSs of different intensities (Cohen et al. 2005). For example, large versus small CAPE could mean a mature versus a weakening MCS *and* a strong versus weak MCS. Therefore, the higher the probability of MCS maintenance, the more likely it is that an MCS will be

maintained *and* be strong, but the relative contribution of the predictors to its maintenance versus its intensity can not be determined in any given case.

The same ambiguity in interpretation of the probabilities applies to the MCS speed probabilities. The logistic regression equation was designed so that predictors that result in y = 0.9 means that the MCS has a 90% chance of having a forward-propagating leading edge that moves at speeds $\geq$ 18 m s^{-1}. But the factors that lead to a fast-forward propagating cold pool also are related to the factors that produce strong systems (Cohen et al. 2005). We believe that this ambiguity in interpretation, however, does not hinder the general application of these equations for particular forecast problems as discussed later in section 5.

4. RESULTS

a. MCS maintenance probabilities

Guided by previous studies that find parameters related to the environmental wind shear profile (Weisman and Rotunno 2004, Coniglio et al. 2004, Parker and Johnson 2004), the mean winds speeds (Evans and Doswell 2001), and the instability to be important for the development and maintenance of robust, quasi-linear MCSs, we first seek to quantify the differences among these parameters between the mature and dissipation soundings (differences in the initiation and mature soundings are found to be small for most parameters).

We first examine many wind shear parameters (bulk shear, total shear, positive versus negative shear) over many different layers of the atmosphere and identify the particular wind shear parameter and layer that best separated the mature and dissipation soundings. Although many of the differences in the wind shear parameters are statistically significant, the greatest differences are found among the shear vector magnitudes (bulk shear) over very deep layers, with the values being larger for the mature soundings (Fig. 5), as suggested for derecho-producing MCSs alone by Coniglio et al. (2004).

The differences are relatively small for the low-level shear magnitudes, suggesting that these values, alone, have limited utility in determining the stage of the MCS lifecycle. Fig. 5 suggests that an integrated measure of shear over a very deep layer will have the most utility in forecasting the weakening of MCSs. Calculations of the total shear, or the hodograph length, support this claim (not shown). The wind shear over a deep layer is perhaps the most promising wind shear variable to use in a forecasting scheme because of the significant influence that mid-upper-level wind shear can have significant influences on the maintenance of MCSs (see section 2) along with the positive influences of the low-

level shear on the initial organization and the strength of the system (Weisman and Rotunno 2004). To account for the possibility of variable heights of the low-level or upper-level jets that often control the effective depth and magnitude of shear, we use the maximum bulk shear between 0-1 km and 6-10 km (this is hereafter referred to as the "maximum shear") as our shear predictor in the logistic regression procedure.
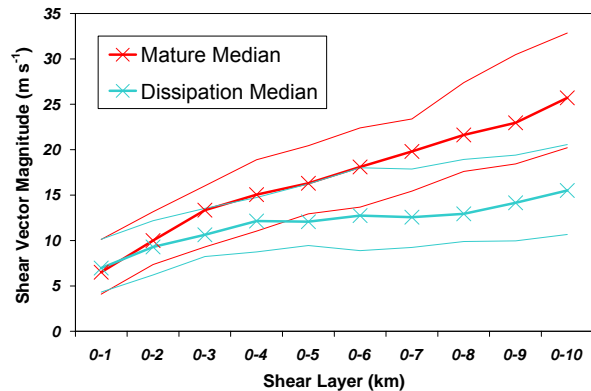

Fig. 5. Median shear vector magnitudes (lines marked X) calculated over various depths among the mature (red) and dissipation (blue) sounding groups. The thin lines enclose the 25th and 75th percentiles of each distribution.

We examined many parameters related to instability, including several variations of CAPE, lapse rates over many layers, vertical differences in θ_e over many layers and find that the lapse rates over a deep portion of the convective cloud layer (generally from the lifting condensation level to some pressure level in the 500 hPa to 300 hPa layer) are found to be the most significantly different among the mature and dissipation soundings. In height coordinates, the 3-8 km lapse rate had the highest Z-score among the two groups, and is thus used as the primary instability variable in the logistic regression equation for MCS maintenance. As illustrated in Fig. 6, a discriminant analysis (Wilks 1995) between the two groups shows that the 3-8 km lapse rate along with the maximum shear separate 75% of the soundings correctly. This suggests that these two parameters alone could be used to forecast the weakening and dissipation of MCSs effectively, but there is no limitation to the number of parameters that can be used in a discriminant analysis or in logistic regression leaving room for improvement.
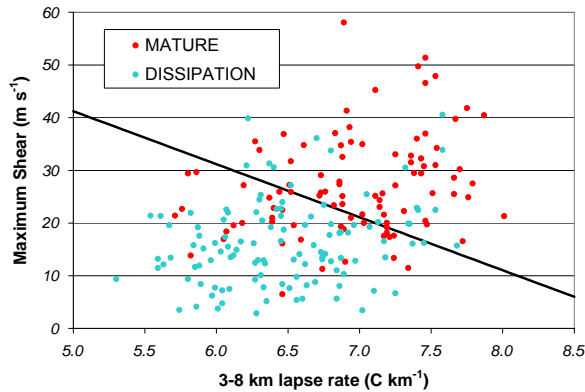
Fig. 6. Scatterplot of the maximum shear (m s⁻¹) versus the 3-8 km lapse rate (C km⁻¹) for the mature and dissipation soundings. The linear discrimination line separates 75% of the soundings correctly.

Among the other instability variables, we find that the distribution of the most unstable parcel CAPE (MUCAPE) had a large Z-score between the mature and dissipation soundings and, interestingly, was only weakly correlated with the 3-8 km lapse rates. This appears to be because the CAPE variables are determined primarily by the absolute moisture content in the layer with the maximum θ_e (not shown). The use of a CAPE variable that isn't tied to a particular level is desirable because this allows for the at least the possibility of including the elevated systems in the discrimination.

In addition, mean wind speeds over a deep layer are significantly different between the mature and dissipation soundings. Despite a moderate correlation with the deep shear values, the deep-layer mean winds are used because they provide an increased ability to discriminate between the mature and dissipation soundings when included with the other three parameters. The 3-12 km mean wind has the largest Z-score and is used as the mean wind predictor.

The four parameters mentioned above (maximum shear, 3-8 km lapse rate, MUCAPE, and 3-12 km mean wind) collectively separate over 80% of the soundings correctly when input into a discriminant analysis. Because of the mutual correlations among the hundreds of variables, any additional parameters are found to provide negligible benefit to discriminate among the two groups. Therefore, the maximum shear (maxshear), 3-8 km lapse rate (3-8 lr), MUCAPE, and 3-12 km mean wind (3-12 mw) are used as predictors in eq. (1) to develop the following equation for the MCS maintenance probability (MMP):

For $MUCAPE \geq 100 \, J \, Kg^{-1}$:

$$MMP = \frac{1}{[1 + EXP(a_0 + (a_1 * \{\max shear\}) + (a_2 * \{3-8\,lr\}) + (a_3 * \{MUCAPE\}) + (a_4 * \{3-12\,mw\}))]}$$

For $MUCAPE < 100 \, J \, Kg^{-1}$:

$$MMP = 0,$$

where the regression coefficients are $a_0 = 13.0$, $a_1 = -4.59 \times 10^{-2}$, $a_2 = -1.16$, $a_3 = -6.17 \times 10^{-4}$, and $a_4 = -0.17$ and the predictors are described above. By design, the application of these probabilities is conditional upon the development of an MCS. Fig. 7 shows a plot of the equation for MMP for the four predictors that are normalized by their respective minimum and maximum values in the data set. The steepness of the curve for MMP suggests the potential for substantial skill in discriminating mature and weakening MCSs.
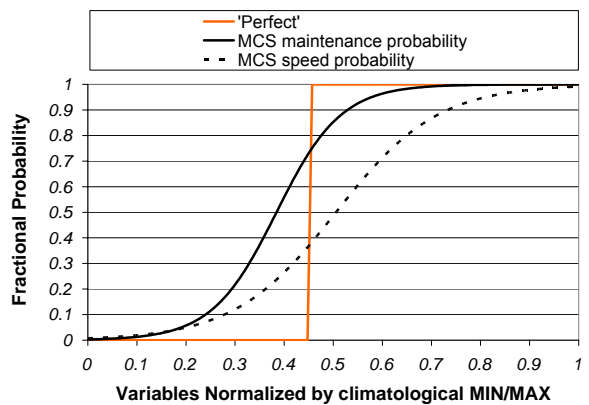
Fig. 7. Probability of MCS maintenance (MMP, solid line) and MCS speed ≥ 18 m s⁻¹ (MSP, dashed line) based on logistic regression. A "perfect" regression (orange line) is shown for reference. The ordinate represents the predictors normalized by their minimum and maximum values in the data set. For example, if all four of the predictors for the equation for MCS maintenance are exactly half way between their min and max values (0.5), then the regression equation predicts a ~90% chance that the MCS will be maintained. In general, a steeper curve means a better ability of the parameters to discriminate between the two groups.

We envision the best real-time application of the MMP would use observational data or short-term model output at a time close to convective initiation. For example, gridded fields from the hourly Rapid Update Cycle (RUC) (Benjamin et al 2003) can be used to calculate these probabilities and give guidance to the regions most likely to sustain strong MCSs that do develop. We reiterate that this could directly benefit Day 1 Severe Weather Outlooks, Mesoscale Discussion products, and the issuance of Severe Weather Watches at the Storm Prediction Center (SPC) and short-term forecasts issued by local forecast offices.

Additionally, although the MMP is designed to discriminate between mature and dissipating MCSs that

are imminent or ongoing, it may also be used with mesoscale model output well before convective initiation to give a general idea of where strong, quasi-steady mature MCSs may be favored on longer time scales (assuming convection in the model doesn't remove instability erroneously).

b. MCS speed probabilities (MSP)

The same procedure described in Section 3 is followed using the soundings in the $C < 18$ m s^{-1} and $C \geq 18$ m s^{-1} groups to identify the parameters that best discriminate between the two groups. Through significance testing and discriminant analysis, it is found that the low- to upper-level mean wind speeds discriminates between the two groups the best. Wind shear over deep layers (> 5 km deep) also discriminated well between the two groups, but not as well as the mean wind variables. This may suggest that the mean wind speed, and its effects on the cold pool motion, has a more direct impact on the MCS forward-speed than the effects of the deeper wind shear, as suggested by Evans and Doswell (2001). The mean wind speed calculated over the 2-12 km layer has the highest Z-score, and thus is chosen to be the kinematic predictor variable for the development of the probability equation.

Interestingly, for the thermodynamic variables, the Z-scores are much smaller for all of the variables compared to the kinematics variables, including CAPE, mean low-level mixing ratios, lapse rates, and vertical differences in θ_e, and thus, they do not provide a good discrimination between the two groups. However, by grouping the data according to geographical regions, it is found that the geographical signal in the data is very large. For example, for the cases for which $C \geq 18$ m s^{-1}, the lapse rates and vertical shear parameters are much smaller for the cases east of the Mississippi River compared to the high-plains events. The converse is true for the precipitable water values and the mean mixing ratio in the lowest few kilometers, as would be expected given the proximity to the Gulf of Mexico moisture source. These differences in the parameters are large enough so that the parameters can't discriminate between the MCS speed categories when combined into the groups that combine all geographical locations east of the Rocky Mountains.

It is interesting that when the variables are converted into non-dimensional standard normal variables (Wilks 1995) based on their 7-year (1998-2004) mean and standard deviation derived from radiosonde data, the parameters are much better able to discriminate between the two MCS speed categories. This conversion to standard normal variables provides a means to identify parameters that can be used effectively in the development of the MCS speed probabilities, as described next.

Among the normalized variables, the maximum low-to mid-level difference in θ_e and the lapse rate in the lower half of the convective cloud layer were found to discriminate between the two groups very well. Based on these findings, the normalized maximum vertical difference in θ_e between low and mid levels (maxthediff´), the 2-12 km mean wind speed (m s^{-1}) (2-12 mw), and the normalized 2-6 km lapse rate (2-6 lr´) are used as predictors in eq. (1) to generate an equation for the conditional probability that an MCS will move with speeds ≥ 18 m s^{-1} at maturity, and is given by,

$$\underline{For\ MUCAPE \geq 100\ J\ Kg^{-1}:}$$

$$MSP = \frac{1}{\left[1 + EXP(a_0 + (a_1 * \{\max thediff\,''\}) + (a_2 * \{2-12\ mw\}) + (a_3 * \{2-6\ lr'\}))\right]}$$

$$\underline{For\ MUCAPE < 100\ J\ Kg^{-1}:}$$

$$MSP = 0$$

where the regression coefficients are $a_0 = -3.46$, $a_1 = 0.447$, $a_2 = 0.119$, and $a_3 = 0.79$ and the predictors are defined above. Although the regression curve for MSP is not as steep as the curve for MMP (Fig. 7), indicating a lesser degree of statistical difference between the two groups, the slope of the curve still suggests the ability to discriminate between "slow" and "fast" MCSs, and perhaps, give an indication of the likelihood for the occurrence of a severe-wind producing MCS.

5. APPLICATION AND DISCUSSION

As part of the NOAA Hazardous Weather Testbed, a small collaborative program recently took place during the summer of 2005 at the SPC and the National Severe Storms Laboratory (NSSL) to test the ability of these conditional probability forecasts to provide useful guidance on the speed and dissipation of forward-propagating MCSs (see http://www.spc.noaa.gov/exper/Summer_2005 for more information). To meet the goals of this program, daily activities included the documentation of MCSs using national mosaic radar reflectivity and the evaluation of the probabilities calculated using the hourly RUC forecasts.

Examples of the MMP and MSP generated from operational RUC model output are illustrated for a derecho MCS event hat occurred on 2-3 July 2005 (Fig. 8). The MCS developed a broad bowing signature in its early stages and was composed of smaller-scale bow echoes that were responsible for several reports of wind gusts > 65 kts in western South Dakota. The wind reports became less frequent as the MCS expanded in size and the leading line exhibited less bowing characteristics after 0700 UTC. During its lifetime, the MCS moved at speeds of 40-45 kts (20-22 m s^{-1}), but slowed to around 30-35 kts in the last few hours of its existence, which coincided with a general weakening of the 50+ dBZ echoes within the leading line.
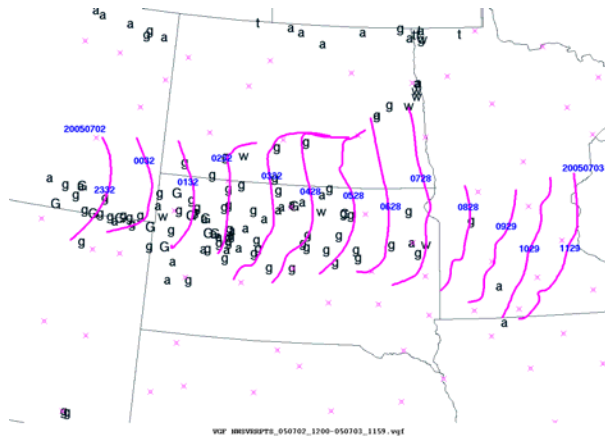
Fig. 8. Hourly traces of the leading edge of the nearly contiguous area of 35+ dBZ echoes associated with the MCS on 2-3 July 2005 (pink lines). Times (UTC) of the traces are labeled in blue and the dates (YYYYMMDD) are shown for the first and last trace. The letters represent severe weather reports from 1200 UTC on 2 July 2005 to 1159 UTC on 3 July 2005 (g – severe wind gust, w- severe wind, a – severe hail, t – tornado). Capital letters represent "significant" reports (65+ kt wind or 2+ in hail).

The RUC forecasts generate MMPs over 90% in the region of the MCS for much of its lifecycle (Fig. 9a). The area of the MMP contours change little throughout the 12 h forecast cycle so that the 3 h forecasts of MMP provide a good representation of the fields at the other forecast hours. The MMP appears to indicate that the northern half of the MCS would begin to weaken after 0800 UTC as the probabilities decrease to 30-40% in western and north-central Minnesota. it also suggests the MCS dissipation in southeastern Minnesota as a large east-west gradient in the probabilities is found in this area.

The MSPs also suggest the persistence of a favorable environment for the system to attain speeds > 35 kts as the MSPs were 60-70% in much of the area that the MCS traversed (Fig. 9b). In addition, the MSPs drop to 20-30% where the system slowed to speeds < 35 kts over southern Minnesota toward the end of its lifecycle.
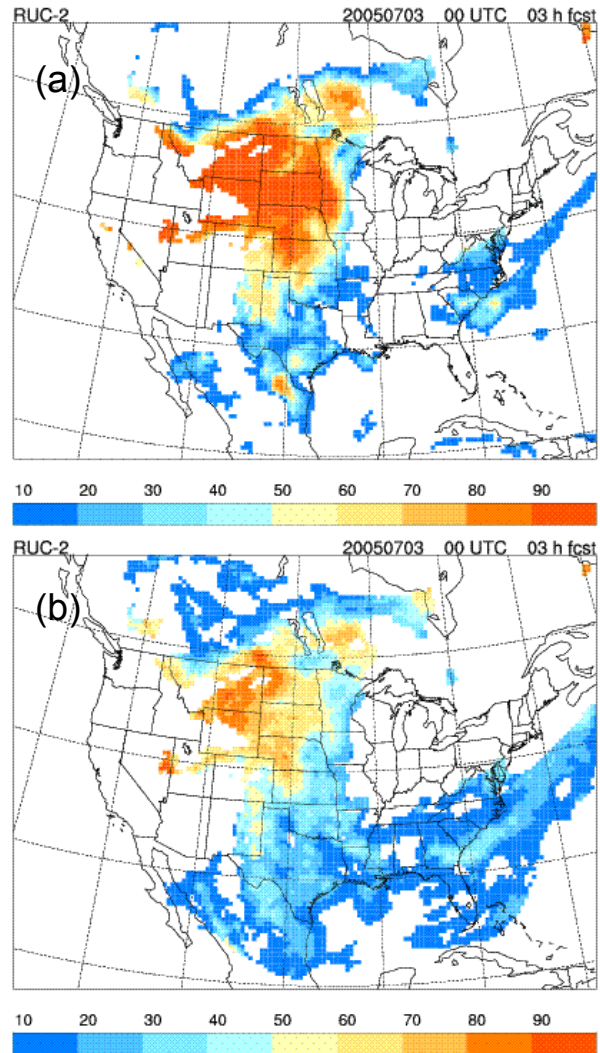

Fig. 9. (a) Values of the MCS maintenance probability (%) based on a 3-h RUC forecast valid at 0300 UTC 3 July 2005. (b) As in (a), except for the probability of MCS speed ≥ 18 m s^{-1}(%).

The above example illustrates a successful application of the MMP and MSP probabilities with short-term numerical model output. Although the analyses of the data collected during the SPC/NSSL Summer Program are very preliminary at the time of this writing, the equations appear to provide useful guidance on the transition of system with a solid line of 50+ dbZ echoes to a more disorganized system with unsteady changes in structure and propagation characteristics. We also see indications that the equations can help to determine whether or not an MCS will produce severe surface winds, which is somewhat surprising since the production of convectively-induced surface winds often depends on the meso-α scale details of the low-level thermodynamic environment, which are not likely to be

represented well on the 40-km RUC grid. This speaks to the potential of these probability equations to particular forecast problems, despite the ambiguity in the interpretation of the equations discussed at the end of section 3.

The belief that the equations provide useful guidance on the potential for an MCS to produce severe surface winds will be explored in detail a future paper, but this point is briefly illustrated here with a supercell/MCS event that occurred between 0000 - 1400 UTC on 1 July 2005 in the central and southern Plains region (Fig. 10). A nearly-stationary synoptic frontal boundary meandered from the front range of the Colorado Rockies southward into far northeastern New Mexico, then stretched eastward across the Texas panhandle region and eventually northeastward toward the central Mississippi river valley. Isolated convection initiated in east-central Colorado during the late afternoon of 30 June and developed into an elevated supercell that moved through southeastern Colorado and southwestern Kansas from 0200 to 0600 UTC (Fig. 10). Despite a 150 hPa deep frontal zone observed in the 0000 UTC Dodge City sounding (not shown), severe surface winds were reported with the upscale growth of the supercell with wind gusts estimated up to 80 knots across the region. The supercell then continued to grow upscale and developed linear characteristics as it entered Oklahoma, with a continuation of the severe surface winds north of the front.
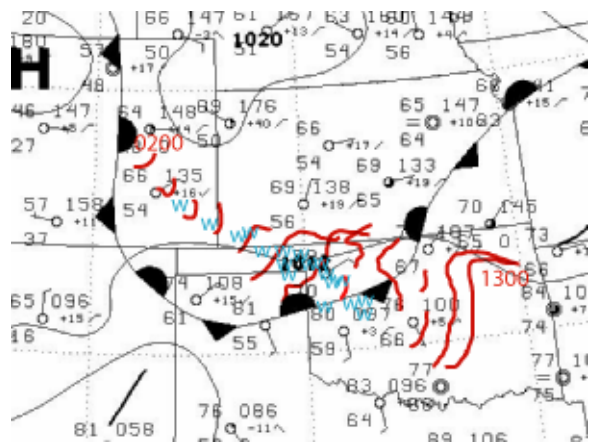

Fig. 10. NCEP surface chart valid 0600 UTC on 1 July 2005. Red lines denote the hourly positions of the leading edge of the 50+ dbz echoes associated with the supercell and MCS from 0200 UTC to 1300 UTC. The blue W's denote the locations of severe wind reports.

However, it is interesting that the system stopped producing severe winds as it crossed the front into the warm sector air (Fig. 10). The line underwent changes in structure and showed characteristics of discrete forward propagation during this period, but once the system cleared the frontal zone and moved into central Oklahoma, the system reorganized into a solid, albeit,

weaker linear system. The persistence and strength of the surface winds north of the surface frontal boundary and the cessation of the severe winds once the convective system expanded and crossed into the warm sector (Fig. 10) was not anticipated with this event as it was assumed the boundary layer north of the front was too deep to support the penetration of strong downdrafts to the surface.

Since there was substantial elevated CAPE and the shear and the lapse rates in the depth of the convective cloud layer were relatively large, the MMP values based on the 9-h RUC forecast suggested the persistence of a strong, quasi-linear system through southwestern Kansas and Northwestern Oklahoma with values of 70-90% in the region that supported the supercell to MCS transition (Fig. 11). The MMP values also suggested a weakening system across central Oklahoma with values dropping quickly to 10-20%. It is intriguing that the relatively confined region of high MMP values also coincided with the regions that experienced the severe surface winds. This provides hope that these empirical techniques can also be applied to the prediction of severe elevated systems with some confidence (as they were designed to do), in addition to providing useful guidance on more surface-based systems (Figs. 8 and 9).
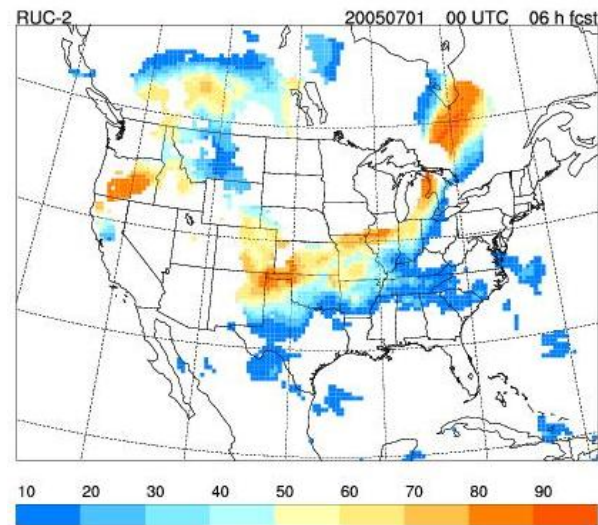
Fig. 11. (a) Values of the MCS maintenance probability (%) based on a 6-h RUC forecast valid at 0600 UTC 1 July 2005.

We are also mindful of limitations of the probability equations and in the use of cold pool/shear/mean wind concepts for the forecasting of MCSs in general. In retrospect, we have shown that once MCSs become established, the deeper layer wind shear tends to provide a better indicator of MCS longevity than low-level-only shear parameters and have briefly discussed some of the physical mechanisms for this in section 2. This appears to be especially true of the cases that mature in the stronger shear and larger lapse-rate

regimes typical of the central United States during the warm season. However, the probabilities developed in this paper and these concepts in general will likely work best on MCSs that develop and continually generate strong cold pools away from larger-scale forcing and when the shear and mean winds are substantial. Certainly, MCSs can also maintain coherence through other means including discrete propagation along a surging outflow (see the MCS event on 30 June 2005 in the Ohio valley for this type of event in which the MMP values had little skill), frontogenetic circulations, gravity-wave interactions, and other larger-scale forcing mechanisms. We will report on the overall performance of the equations for the various MCS modes observed during the Summer Program in a future paper.

It should be noted that the tools developed herein are designed with the goals of the SPC in mind, particularly with the issuance of the afternoon Day 1 convective outlooks and the issuance and/or continuance of watches along MCS tracks. We recognize that the convective-scale details of the evolution, especially the low-level vertical thermodynamic structures of the system and the environment, which ultimately dictate the county-scale locations of severe surface winds, likely will await advances in either the ability to observe the fine-scale details of the low-level moisture in real time or advances in the prediction these systems with numerical weather prediction schemes that assimilate convective-scale observations (see Dowell et al. 2004 for an example). But the examples presented above illustrate that forecast tools based on environmental parameters and their statistical relationships still have the potential to provide forecasters with improved information on the qualitative characteristics of the MCS structure and longevity and, perhaps, refined information on the potential for severe weather on regional scales. We urge the meteorological community to continue to undertake studies of this type while we move forward into the era of convective-scale data assimilation into convection-resolving numerical weather prediction models.

6. ACKNOWLEDGMENTS

7. REFERENCES

Benjamin, S.G. and others, 2003: An hourly assimilation-forecast cycle: The RUC. *Mon. Wea. Rev.*, 132, 495-518.

Bryan, G., D. Ahijevych, C.A. Davis, and M.L. Weisman, 2005: Observations of cold pool properties in mesoscale convective systems during BAMEX. Preprints, 32nd Conf. on Mesoscale Meteorology, Amer. Meteor. Soc., Albuquerque, NM, CD-ROM.

Cohen, A.E., M.C. Coniglio, S.F. Corfidi, and S.J. Taylor, 2005: Discriminating among non-severe, severe, and derecho-producing mesoscale convective system environments. Preprints, Severe Local Storms Symposium, Amer. Meteor. Soc., Atlanta, GA, CD-ROM.

Coniglio, M.C., D.J. Stensrud, and M.B. Richman, 2004: An observational study of derecho-producing convective systems. *Wea. Forecasting*, **19**, 320-337.

--------,--------, and L.J. Wicker, 2004: How upper-level shear can promote organized convective systems. Preprints, 22nd conference on Severe Local Storms, Hyannis, MA, 10.5.

--------, L.J. Wicker, and D.J. Stensrud, 2005: Effects of upper-level shear on the structure and maintenance of strong quasi-linear convective systems. *J. Atmos. Sci.*, in press.

Corfidi, S.F., 2003: Cold pools and MCS propagation: Forecasting the motion of downwind-developing MCSs. *Wea. Forecasting*, **18**, 997-1017.

Cotton, W.R., M.-S. Lin, R.L. McAnelly, and C.J. Tremback, 1989: A composite model of mesoscale convective complexes. *Mon. Wea. Rev.*, **117**, 765-783.

Davis, C.A., N. Atkins, D. Bartels, L.F. Bosart, G. Byran, M. Coniglio, W. Cotton, D.Dowell, B.Jewett, R.Johns, D. Jorgensen, J. Knievel, K. Knupp, W. Lee, G. Mcfarquhar, J. Moore, R. Przybylinski, R. Rauber, B. Smull, R. Trapp, S. Trier, R. Wakimoto, M. Weisman and C. Ziegler, 2004: The Bow-Echo and MCV experiment (BAMEX): Observations and Opportunities. *Bull. Amer. Meteor. Soc.,* **85**, 1075-1093.

Dowell, D.C., F. Zhang, L.J. Wicker, C. Snyder, and N.A. Crook, 2004: Wind and temperature retrievals in the 17 May 1981 Arcadia, Oklahoma, supercell: Ensemble Kalman filter experiments. *Mon. Wea. Rev.*, **132**, 1982-2005.

Evans, J.S., and C.A. Doswell, 2001: Examination of derecho environments using proximity soundings. *Wea. Forecasting*, **16,** 329-342.

Fovell, R. G. and P.S. Daily, 1995: The temporal behavior of numerically simulated multi-cell type storms. Part I: Modes of behavior. *J. Atmos. Sci.*, **52**, 2073-2095.

Fritsch J.M. and G.S. Forbes, 2001: Mesoscale convective systems. *Severe Convective Storms*, *AMS Meteor. Monogr.*, C. Doswell III, Ed., **28**, Amer. Meteor. Soc., 323-357.

Gale, J.J., W.A. Gallus Jr., and K.A. Jungbluth, 2002: Toward improved prediction of mesoscale convective system dissipation. *Wea. Forecasting*, **17**, 856-872.

Kain. J.S., S.J. Weiss, M.E. Baldwin, G.W. Carbin, D. Bright, J.J. Levit, and J.A. Hart, 2005: Evaluating high-resolution configurations of the WRF model that are used to forecast severe convective weather: The 2005 SPC/NSSL Spring Experiment. Preprints, 21st conference on Weather Analysis and Forecasting, Amer. Meteor. Soc., Washington, D.C. paper 2A.5.

Moncrieff, M.W. and C. Liu, 1999: Convection initiation by density currents: Role of convergence, shear, and dynamical organization. *Mon. Wea. Rev.*, **127**, 2455-2464.

Parker, M.D., and R.H. Johnson, 2004a: Structures and dynamics of quasi-2D mesoscale convective systems. *J. Atmos. Sci.*, **61**, 545-567.

--------, and --------, 2004b: Simulated convective lines with leading precipitation. Part I: Governing dynamics. *J. Atmos. Sci.*, **61**, 1637-1655.

--------,and --------, 2004c: Simulated convective lines with leading precipitation. Part II: Evolution and maintenance. *J. Atmos. Sci.*, **61**, 1656-1673.

Shapiro, A., 1992: A hydrodynamical model of shear flow over semi-infinite barriers with application to density currents. *J. Atmos. Sci.*, **49**, 2293-2305.

Stensrud D.J., M.C. Coniglio, R. Davies-Jones, and J. Evans, 2005: Comments on " 'A theory for strong long-lived squall lines' revisted ". *J. Atmos. Sci.*, **62**, 2989-2996.

Trier, S.B. and C.A. Davis, 2005: Propagating nocturnal convection within a 7-day WRF-model simulation. Preprints, 32nd Conf. on Mesoscale Processes, Amer. Meteor. Soc., CD-ROM.

Weisman, M.L., and R. Rotunno, 2004: "A theory for strong, long-lived squall lines" revisted. *J. Atmos. Sci.*, **61**, 361-382.

Wilks, D.S., 1995: *Statistical methods in the atmospheric sciences*. Academic Press, p 419-428.

Zipser, K.A, 1982: Use of a conceptual model of the life cycle of mesoscale convective systems to improve very-short-range forecasts. *Nowcasting*, K. Browning, Ed., Academic Press, 191-204.